ETH
Swiss Federal Institute of Technology Zurich

Seminar for Applied Mathematics

Department of Mathematics

Bachelor Thesis Spring semester 2014

**Thomas Haener**

# Numerical Solution of a Coefficient Identification Problem in the Poisson equation

Submission Date: 18.9.2014

Supervisor: Prof. Dr. Ralf Hiptmair

# Abstract

In this Bachelor thesis, the problem of determining the coefficient $q \in Q := \{q \in L^\infty(\Omega) : 0 < \underline{q} \leq q(x) \leq \overline{q} \text{ a.e. in } \Omega\}$ such that it satisfies the Poisson equation

$$\begin{aligned} -\nabla \cdot (q \nabla u) &= f \qquad \text{in } \Omega \\ u &= 0 \qquad \text{on } \partial\Omega \end{aligned}$$

for given inexact data $u^\delta$ (instead of exact data $u$) with $\|u - u^\delta\|_{H^1(\Omega)} \leq \delta$ is analyzed and solved numerically. It is implemented in c++ using the Distributed and Unified Numerics Environment (DUNE).

The origin of the ill-posed nature of this inverse problem is illustrated in 1D. In order to remedy this ill-posedness, Tikhonov regularization is applied together with Morozov's Discrepancy Principle and, instead of trying to minimize the non-convex least-squares Tikhonov functional, the new convex energy functional found in [1] is used.

Experiments performed with this implementation agree with the theory found in [5]: For smooth coefficients a convergence rate of $O(\sqrt{\delta})$ in the $L^2(\Omega)$-Norm is observed and for non-smooth coefficients the reconstruction and the convergence rates are found to be much worse.

# Contents

# Chapter 1

# Introduction

## 1.1 Problem formulation

Let $f \in L^2(\Omega)$ be the load function for the Poisson problem and let $U(q) \in H_0^1(\Omega)$ denote the forward solution for a given coefficient $q \in Q := \{q \in L^\infty(\Omega) : 0 < \underline{q} \leq q(x) \leq \overline{q} \text{ a.e. in } \Omega\}$, i.e. $U(q)$ satisfies

$$\begin{aligned} -\nabla \cdot (q \nabla U(q)) &= f \text{ in } \Omega \\ U(q) &= 0 \text{ on } \partial\Omega \end{aligned}$$

in a weak sense. Then the coefficient identification problem at hand can be rewritten as follows: Given inexact data $u^\delta$ with $\|U(q) - u^\delta\|_Y$ bounded by the noise level $\delta \geq 0$, i.e. $\|U(q) - u^\delta\|_Y \leq \delta$, find $q \in Q$ such that

$$q \in \arg\min_{\tilde{q} \in Q} \|U(\tilde{q}) - u^\delta\|_Y^2$$

### 1.1.1 Ill-posedness (in 1D)

To see that this problem is ill-posed (not well-posed) in the sense of Hadamard (see e.g. [4, Definition 1.5.2]), consider the Poisson equation on $\Omega = [0, 1]$:

$$\begin{aligned} -(q(x)u'(x))' &= f \quad \forall x \in (0,1) \\ u(0) &= u(1) = 0 \end{aligned}$$

Solving for its coefficient yields

$$q(x) = -\frac{F(x)}{u'(x)} \tag{1.1.1.1}$$

where $F(x)$ denotes the indefinite integral of the load function $f(x)$.

Since it is assumed that the noise can be controlled in the $H_0^1(\Omega)$-Norm, there are only small perturbations in $u'(x)$ almost everywhere. Nevertheless, this causes big changes in $q(x)$ w.r.t. the $L^2(\Omega)$-Norm, resulting from neighborhoods where $u'(x)$ is small. From $u(0) = u(1) = 0$ it follows that $u'(x) = 0$ somewhere, and, in a neighborhood of this $x$, $u'(x)$ is small.

Note that, in the absence of noise, the constant of the indefinite integral can (and must) be chosen such that the singularity cancels.

**Example.** Let $f(x) = 1$ and $q(x) = 1$. Then

$$\begin{aligned}(q(x)u'(x))' &= -f \\ u'(x) &= -x + B \\ u(x) &= -\frac{1}{2}x^2 + Bx + C\end{aligned}$$

Using that $u(0) = u(1) = 0$, one finds that $D = 0$ and $C = \frac{1}{2}$. Applying the solution formula (1.1.1.1) to this $u(x) = \frac{1}{2}x(1-x)$ yields

$$q(x) = \frac{F(x)}{u'(x)} = \frac{-x + A}{-x + \frac{1}{2}}$$

where $A = \frac{1}{2}$ in order to have that $q(x) \in Q \subset L^\infty(\Omega)$.

There is only one constant that can be chosen such that a singularity is canceled, but when noise is introduced there may be several zeros of $u'(x)$, which implies ill-posedness.

### 1.1.2 Regularization

Since the problem at hand is an (ill-posed) inverse problem, regularization is needed in order to get useful results. In this thesis, the functional to be minimized is regularized by applying *Tikhonov regularization*, as discussed in [1] and [4, Section 7.4]. The resulting minimization problem looks as follows:

Find $q \in Q$ such that

$$q \in \arg\min_{\tilde{q} \in X} \frac{1}{2}\|U(\tilde{q}) - u^\delta\|_Y^2 + \frac{\alpha}{2}\|\tilde{q} - q^\star\|_Q^2 \tag{1.1.2.1}$$

where $q^\star$ is a guess for $q$, $0 < \alpha \in \mathbb{R}$ is the regularization parameter. Since the measurement error can be controlled in the $H^1(\Omega)$-Norm, (1.1.2.1) is valid for $Y := H_0^1(\Omega)$.

The mapping

$$\mathcal{R}_\alpha : Y \to Q$$

which maps a given $u^\delta \in Y$ to $q \in Q$, such that (1.1.2.1) is minimized, defines a *reconstruction operator*.

### 1.1.3 Morozov's Discrepancy Principle

Determining the regularization parameter $\alpha$ of a reconstruction operator $\mathcal{R}_\alpha$ correctly is crucial in order to get good reconstruction results. One way to do so is called *Morozov's Discrepancy Principle* found in [4, Section 3.5]:

Let $\tau > 1$ be a safety parameter, $\delta$ the noise-level i.e. $\|U(q) - u^\delta\|_Y \leq \delta$, and $\mathscr{A}$ the set of valid parameters. Then

$$\alpha_{\text{d.p.}} := \sup\{\alpha \in \mathscr{A} : \|U(\mathcal{R}_\alpha(u^\delta)) - u^\delta\|_Y \leq \tau\delta\}$$

where $U : Q \to Y$ denotes the forward operator.

In this thesis, Tikhonov regularization together with the Discrepancy Principle is used to solve the inverse coefficient problem.

# Chapter 2

# Theory

## 2.1 Forward Operator (Poisson Equation)

The mapping $U : Q \to Y$, which maps a given coefficient $q \in Q := \{q \in L^\infty(\Omega) : 0 < \underline{q} \leq q(x) \leq \overline{q} \text{ a.e. in } \Omega\}$ to a weak solution $u \in Y$ of

$$\begin{aligned} -\nabla \cdot (q\,\nabla u) &= f \qquad \text{in } \Omega \\ u &= 0 \qquad \text{on } \partial\Omega \end{aligned} \tag{2.1.0.1}$$

is called the *forward operator*. The weak formulation of the problem looks as follows:

$$-\langle \nabla \cdot (q\nabla u), v\rangle_{L^2(\Omega)} = \langle f, v\rangle_{L^2(\Omega)} \;\; \forall v \in V := H_0^1(\Omega)$$

where $V$ denotes the test function space. When applying Greens First Identity and making use of the fact that $v = 0$ on $\partial\Omega$, the integral over the boundary vanishes, yielding the following reformulated problem:

Find $u \in Y := H_0^1(\Omega)$ such that

$$a(u,v) := \int_\Omega q(x)\nabla u \nabla v\, dx = \int_\Omega fv\, dx =: l(v) \;\; \forall v \in V := H_0^1(\Omega) \tag{2.1.0.2}$$

Clearly, the bilinear form $a : H_0^1(\Omega) \times H_0^1(\Omega) \to \mathbb{R}$ is symmetric and positive definite. Assuming that $f \in L^2(\Omega)$ and $q \in Q$,

$$\begin{aligned} |l(u)|^2 &= \left| \int_\Omega fu\, dx \right|^2 \\ &\leq \int_\Omega f^2\, dx \int_\Omega u^2\, dx && \text{(Cauchy-Schwarz)} \\ &= \|f\|^2_{L^2(\Omega)} \|u\|^2_{L^2(\Omega)} \leq C\|\nabla u\|^2_{L^2(\Omega)} && \text{(Poincaré-Friedrichs)} \\ &\leq \frac{C}{\underline{q}} a(u,u) \end{aligned}$$

Therefore, $l(u)$ is a continuous linear functional on $\Omega$ with respect to the norm induced by $a(\cdot,\cdot)$. According to Theorem 2.3.13 in [2], this implies existence and uniqueness of the solution.

## 2.2 Minimization of the functional: Adjoint method

Finding the solution of the inverse coefficient problem at hand can be recast into the form of an equality constrained minimization problem found in [3, Section 1.6]

$$\begin{aligned} &\min_{(u,q)\in Y\times Q} J(u,q) \\ &\text{s.t. } e(u,q) = 0 \end{aligned}$$

where $e(u,q) := -\nabla\cdot(q(x)\nabla u(x)) - f$ and $q \in Q$ for the Poisson equation.

The numerical solution of such a problem requires the gradient of the functional $J(u,q)$ with respect to the model parameter $q$. One method for computing this gradient is the *adjoint-state method*, which will be discussed here. In [3, Section 1.6.2], the derivation of the adjoint problem and the computation of the gradient is given as follows:

Let $\hat{J}(q) := J(U(q),q)$ denote the reduced functional, $Q^\star$ the dual space of $Q$, and $e(u,q)^\star$ the adjoint of $e(u,q)$. Then

$$\begin{aligned} \langle \hat{J}'(q), s\rangle_{Q^\star,Q} &= \langle J_U(U(q),q), U'(q)s\rangle_{Y^\star,Y} + \langle J_q(U(q),q), s\rangle_{Q^\star,Q} \\ &= \langle U'(q)^\star J_U(U(q),q), s\rangle_{Q^\star,Q} + \langle J_q(U(q),q), s\rangle_{Q^\star,Q} \end{aligned}$$

Making use of the linearity of $\langle\cdot,\cdot\rangle$, this yields

$$\hat{J}'(q) = U'(q)^\star J_U(U(q),q) + J_q(U(q),q)$$

Using that $e(U(q),q) = 0$ by construction and differentiating one gets

$$e_U(U(q),q)U'(q) + e_q(U(q),q) = 0$$

Therefore, $U'(q) = -e_U(U(q),q)^{-1}e_q(U(q),q)$ and

$$\hat{J}'(q) = e_q(U(q),q)^\star e_U(U(q),q)^{-\star}\left(-J_U(U(q),q)\right) + J_q(U(q),q)$$

By defining $p(q)$ as the solution to the equation

$$e_U(U(q),q)^\star p = -J_U(U(q),q) \tag{2.2.0.3}$$

the authors of [3] arrive at

$$\hat{J}'(q) = e_q(U(q),q)^\star p(q) + J_q(U(q),q)$$

where (2.2.0.3) is called the *adjoint problem*.

## 2.3 Adjoint Problem and Gradient Computation

### 2.3.1 Adjoint Problem

As can be seen above, the adjoint problem reads

$$e_U(U(q),q)^\star p = -J_U(U(q),q)$$

where, in this case,

$$e(u,q) := -\nabla \cdot (q(x)\nabla u(x)) - f$$
$$J(u,q) := \frac{1}{2}\|u-u^\delta\|_Y^2 + \frac{\alpha}{2}\|q-q^\star\|_Q^2$$

and the weak formulation for $e(u,q)$ is

$$\langle e(u,q), v\rangle_{L^2(\Omega)} = \langle q(x)\nabla u, \nabla v\rangle_{L^2(\Omega)} - \langle f, v\rangle_{L^2(\Omega)} = 0 \ \ \forall v \in H_0^1(\Omega)$$

Using that the derivative of $e(U(q),q)$ w.r.t. $U$ is $e_U(U(q),q)h = -\nabla\cdot(q(x)\nabla h)$ and since

$$\begin{aligned}\langle e_U(U(q),q)h, v\rangle_{L^2(\Omega)} &= \langle -\nabla\cdot(q(x)\nabla h), v\rangle_{L^2(\Omega)}\\ &= \langle q(x)\nabla h, \nabla v\rangle_{L^2(\Omega)}\\ &= \langle h, e_U(U(q),q)v\rangle_{L^2(\Omega)} \ \ \forall v \in H_0^1(\Omega)\end{aligned}$$

one sees that it is self-adjoint.

For the second term, one gets

$$J(U(q),q) = \frac{1}{2}\langle U(q)-u^\delta, U(q)-u^\delta\rangle_Y + \frac{\alpha}{2}\langle q-q^\star, q-q^\star\rangle_Q$$
$$J_U(U(q),q)h = \langle U(q)-u^\delta, h\rangle_Y$$

In summary, the adjoint problem reads: Find $p \in H_0^1(\Omega)$ such that

$$\int_\Omega q(x)\nabla p\nabla v\,dx = -\langle U(q)-u^\delta, v\rangle_Y \ \ \forall v \in H_0^1(\Omega) \tag{2.3.1.1}$$

### 2.3.2 Gradient Computation

In order to calculate $\hat{J}'(q)$, two more terms are required: $e_q(u,q)^\star$ and $J_q(u,q)$.

$$e_q(u,q)h = -\nabla\cdot(h\nabla u)$$
$$J_q(u,q)h = \alpha\langle q-q^\star, h\rangle_X$$

The adjoint of the first term is found as follows

$$\begin{aligned}\langle e_q(u,q)^\star h, v\rangle_{L^2(\Omega)} &= \langle h, e_q(u,q)v\rangle_{L^2(\Omega)}\\ &= \langle \nabla h, v\nabla u\rangle_{L^2(\Omega)}\\ &= \langle \nabla h\nabla u, v\rangle_{L^2(\Omega)}\end{aligned}$$

In summary, the following two subproblems have to be solved in order to calculate the gradient of the functional:

1. Solve the adjoint problem (2.3.1.1), i.e. find $p(x)$
2. Calculate $\hat{J}'(q)h = \langle \nabla p\nabla u, h\rangle_{L^2(\Omega)} + \alpha\langle q-q^\star, h\rangle_X$

## 2.4 Energy Functional

Since the task of minimizing a non-convex functional is difficult, a convex alternative to the standard least-squares functional is used, namely the energy functional from [1] together with Tikhonov regularization:

$$\hat{J}(q) = \frac{1}{2}\int_\Omega q(x)|\nabla(U(q) - u^\delta)|^2 dx + \frac{\alpha}{2}\|q - q^\star\|^2_{L^2(\Omega)} \tag{2.4.0.1}$$

In [1], Háo and Quyen prove that the energy functional is convex on the set $Q := \{q \in L^\infty(\Omega) : 0 < \underline{q} \leq q(x) \leq \overline{q} \text{ a.e. on } \Omega\}$. Furthermore, they prove that the Tikhonov functional (2.4.0.1) is strictly convex and has a unique minimizer on $Q$. They even give a proof for the following theorem (Theorem 2.3 in [1]):

**Theorem 2.4.0.1.** *Assume that there exists a function $w^\star \in H^{-1}(\Omega)$ such that $q - q^\star = U'(q)^\star w^\star$. Then*

$$\|q^\delta_\alpha - q\|_{L^2(\Omega)} = O(\sqrt{\delta}) \text{ and } \|U(q^\delta_\alpha) - u^\delta\|_{L^2(\Omega)} = O(\delta)$$

*as $\alpha \to 0$ and $\alpha \sim \delta$.*

stating that under the source condition above, a convergence of the regularized solution with noisy data $u^\delta$ to the real solution $q$ is guaranteed to occur at a rate of $O(\sqrt{\delta})$ as $\delta \to 0$.

Using this functional (instead of the least-squares functional) introduces a small change in the gradient computation; namely from using the $H^1(\Omega)$-Norm for the right-hand side of the adjoint problem to using the Energy norm, defined as

$$\|u\|^2_a := a(u, u)$$

where $a(\cdot, \cdot)$ is the bilinear form of the weak formulation of the forward problem (2.1.0.2). Therefore, the adjoint problem now reads

Find $p \in H^1_0(\Omega)$ such that

$$a(p, v) = -a(U(q) - u^\delta, v) \;\; \forall v \in H^1_0(\Omega)$$

and the adjoint solution is simply $p = u^\delta - U(q)$.

# Chapter 3

# Implementation

## 3.1 Forward Operator

The discrete forward operator $U_N : Q \to Y_N$, which maps a given coefficient $q \in Q$ to the solution $u_N \in Y_N$ satisfying the weak formulation (2.1.0.2) of the Poisson equation, was implemented using P1 finite elements on a triangular mesh $\mathscr{M}_N$. Let $\mathscr{B}_N = \{b_N^1, ..., b_N^N\}$ denote the basis. Together with the weak formulation one gets the stiffness matrix $A \in \mathbb{R}^{N \times N}$:

$$A_{ij} = \int_\Omega q(x) \nabla b_N^j(x) \nabla b_N^i(x) dx$$

and the right-hand side vector $\varphi \in \mathbb{R}^N$:

$$\varphi_i = \int_\Omega f(x) b_N^i(x) dx$$

Instead of looping over the nodes and integrating over all adjacent entities of co-dimension 0, the loop is done over the co-dimension 0 entities. When the integration over one element is done, the contributions are distributed to the corresponding nodes, making the assembly much more efficient since each element is considered only once.

This way of doing the assembly is why one needs the local matrix for entity $K \in \mathscr{M}_N$, which was found in [2, Section 3.6]

$$A_{ij}^K = \int_{\hat{K}} D\Phi^{-1} q(\Phi(\hat{x})) D\Phi^{-T} \nabla \hat{b}_N^j \nabla \hat{b}_N^i |\det D\Phi| d\hat{x}$$

where $\hat{(\cdot)}$ denotes $(\cdot)$ on the reference element and $\Phi : \hat{K} \to K$ defines the mapping from the reference triangle $\hat{K}$ to $K$.

This mapping and the underlying mesh are accessed through the Dune interface, allowing for a flexible use of different grid implementations. The resulting linear system of equations is solved using the Pardiso linear solver (PARDISO 5.0.0 Solver Project: http://www.pardiso-project.org/).

## 3.2 Coefficient estimation

The coefficient $q \in Q$ was discretized using a P1 finite element approximation as well. Let $q_N(x) \in Q_N$ denote the finite dimensional approximation of $q(x)$ and $b_N^i(x) \in \mathscr{B}_N$, $i =$

$1, ..., N$ the P1 finite element basis functions. Then

$$q_N(x) = \sum_{i=1}^{N} \nu_i b_N^i(x),\ \nu_i \in \mathbb{R}$$

Therefore, the $N$ coefficients $\nu_i \in \mathbb{R}$ have to be found by minimizing the Tikhonov functional with the correct Tikhonov parameter $\alpha_{\text{d.p.}}$ satisfying the Discrepancy Principle. This is done by choosing $\alpha_0 = 1$ as an initial value and then, in each iteration $i$, minimizing the Tikhonov functional with $\alpha_i = \rho \cdot \alpha_{i-1}$, $\rho \in (0, 1)$, until the Discrepancy Principle is fulfilled for $\alpha_i = \alpha_{\text{d.p.}}$.

The minimization of the Tikhonov functional is done using a nonlinear conjugate gradient method using the Armijo-Goldstein rule for the inexact line search algorithm. Since it may happen that $q_N \notin Q_N$ during the iteration procedure, the method found in [3, Section 2.2.2] is used: $q_N$ is projected onto $Q_N$ prior to evaluating the functional to be minimized. This guarantees a valid forward solution for all iterates.

Solving this problem directly on a fine mesh is not feasible without having a good a priori guess of the Tikhonov parameter $\alpha$ available, since finding the minimizer of the Tikhonov functional for a given $\alpha > 0$ is very time consuming and the search for $\alpha_{\text{d.p.}}$ requires many converged CG runs. Therefore, an iterated mesh-refinement approach is used: The full problem (finding $\alpha_{\text{d.p.}}$ and the corresponding minimizer $q_N \in Q_N$) is solved on a coarse mesh $\mathscr{M}_N$. Then the solution $q_N$ is projected onto the refined mesh (using the embedding of the finite element spaces). If necessary, the Tikhonov parameter is adapted until the Discrepancy Principle is satisfied again. This process is carried out repeatedly, until a sufficiently fine mesh has been reached.

The basic outline of the program (in pseudo-code) looks as follows:

```
function q = findCoefficient(noise_level, u_measured)
        alpha=1;
        q=qguess;
        for refined=1:totalRefinementSteps
                Mesh.refine();
                # project q onto the new (finer) mesh; start minimization there
                q=projectToMesh(q, Mesh);

                while !( residual ~ tau*delta )
                        # start iteration with q from previous step and minimize
                            the functional:
                        [residual, q]=minimizeFunctional(Mesh, q, alpha, u_
                            measured, qguess);
                        # adjust regularization parameter based on residual
                        alpha*=alphaFactor(residual, tau*delta);
                end
        end
        return q;
end
```

Listing 3.1: Program in pseudo-code

Where u_measured $:= u^\delta$ is found by adding noise to the exact solution $U(q_{exact})$ on the finest mesh and then projecting it onto the coarser meshes.

# Chapter 4

# Experiments

In order to test the implementation, several experiments were performed. The performance of the Discrepancy Principle ($\tau = 2.5$) with respect to convergence in the noise level will be analyzed next. Furthermore, the quality and convergence of reconstructions of coefficients of different smoothness will be assessed in a quantitative and qualitative manner. Finally, the effect of using an $H^1(\Omega)$-Tikhonov term instead of the $L^2(\Omega)$-term is studied.

In the following experiments $f = 1$ is used as a load function for the Poisson problem unless stated otherwise.

## 4.1 Convergence in the noise level

One expects a convergence rate of $O(\sqrt{\delta})$ in the $L^2(\Omega)$-Norm as $\delta \to 0$ if the assumption in (2.4.0.1) is satisfied. To determine the regularization parameter $\alpha > 0$, the Discrepancy Principle is used, which, according to [5], can give a convergence rate of $O(\sqrt{\delta})$ if the sought coefficient satisfies a smoothness assumption. The following two experiments were conducted in order to demonstrate this.

### 4.1.1 High-regularity coefficient

Firstly, a coefficient with high regularity, namely

$$q(x) = 0.5 + 0.2 \cdot \cos(4\pi \|R\|), \text{ where } R := (x_1 - 0.3, x_2 - 0.5)^T$$

with an initial guess $q_{guess}(x) = 0.6$ shall be considered on $\Omega = [0,1]^2$ using a triangular mesh with $N = 33'025$ nodes. The program was run at different noise levels $\delta$ in order to investigate the convergence of $q_\alpha^\delta$ to the exact solution $q$ in the $L^2(\Omega)$-Norm.

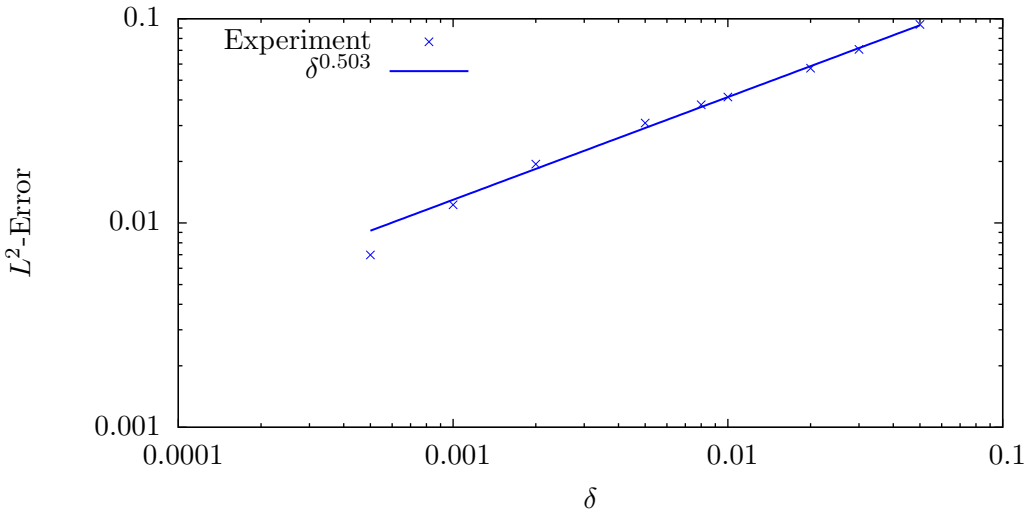


Figure 4.1: High regularity: Convergence in $L^2(\Omega)$

The convergence is exactly as expected. Also, even with 5% of noise added to the forward solution, the qualitative reconstruction of the coefficient is quite good:

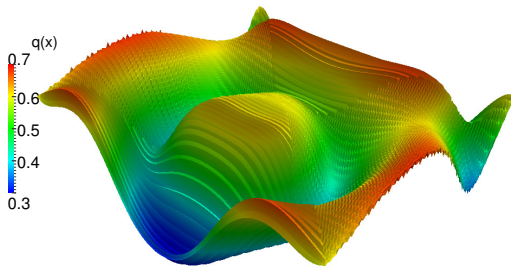


(a) 5% Noise

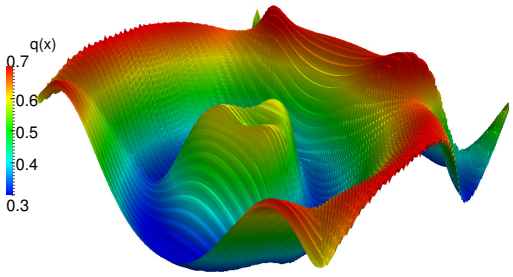


(b) 1% Noise

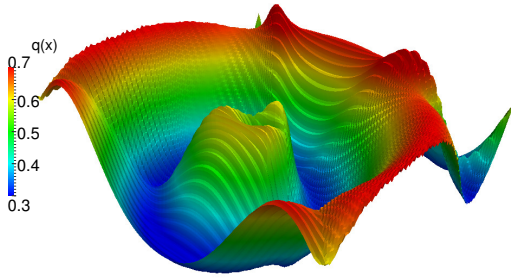


(c) 0.5% Noise

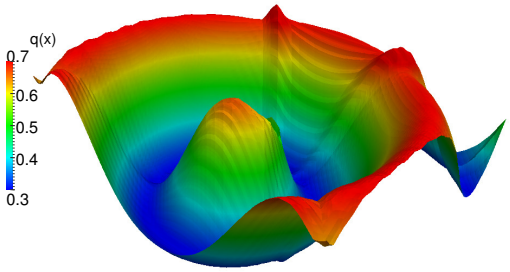


(d) 0.1% Noise

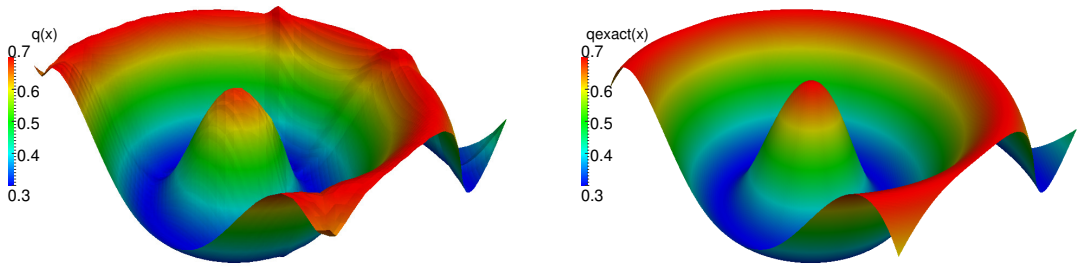


(a) 0.05% Noise (b) Exact $q(x)$

Figure 4.3: Exact and reconstructed solutions for different noise levels

### 4.1.2 Low-regularity coefficient

Next, convergence to a solution with less regularity is investigated. This time, the following coefficient is used:

$$q(x) = \begin{cases} 0.8 & \text{, if } x \in [0.5, 0.7]^2 \\ & \text{or } x \in [0.1, 0.3]^2 \\ & \text{or } x \in [0.1, 0.2] \times [0.8, 0.9] \\ 0.5 & \text{, else} \end{cases}$$

The calculations are performed on the same mesh as before, in order to be able to compare the reconstruction process of a low-regularity coefficient to one of a high-regularity coefficient. Also, the same noise levels $\delta$ are used.

The $L^2(\Omega)$-convergence in this case looks as follows:

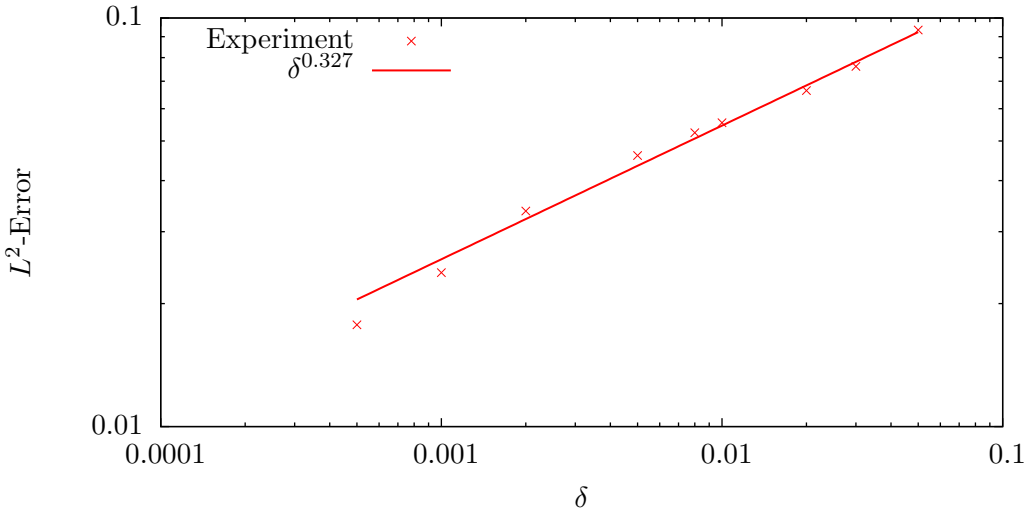


Figure 4.4: Low regularity: Convergence in $L^2(\Omega)$

One can clearly see that the low regularity of the solution has a big impact on the convergence rate in the noise level. The rate went from 0.5 down to 0.33, which is quite drastic. This can also be observed qualitatively in the following 3D plots of the reconstructed solutions:

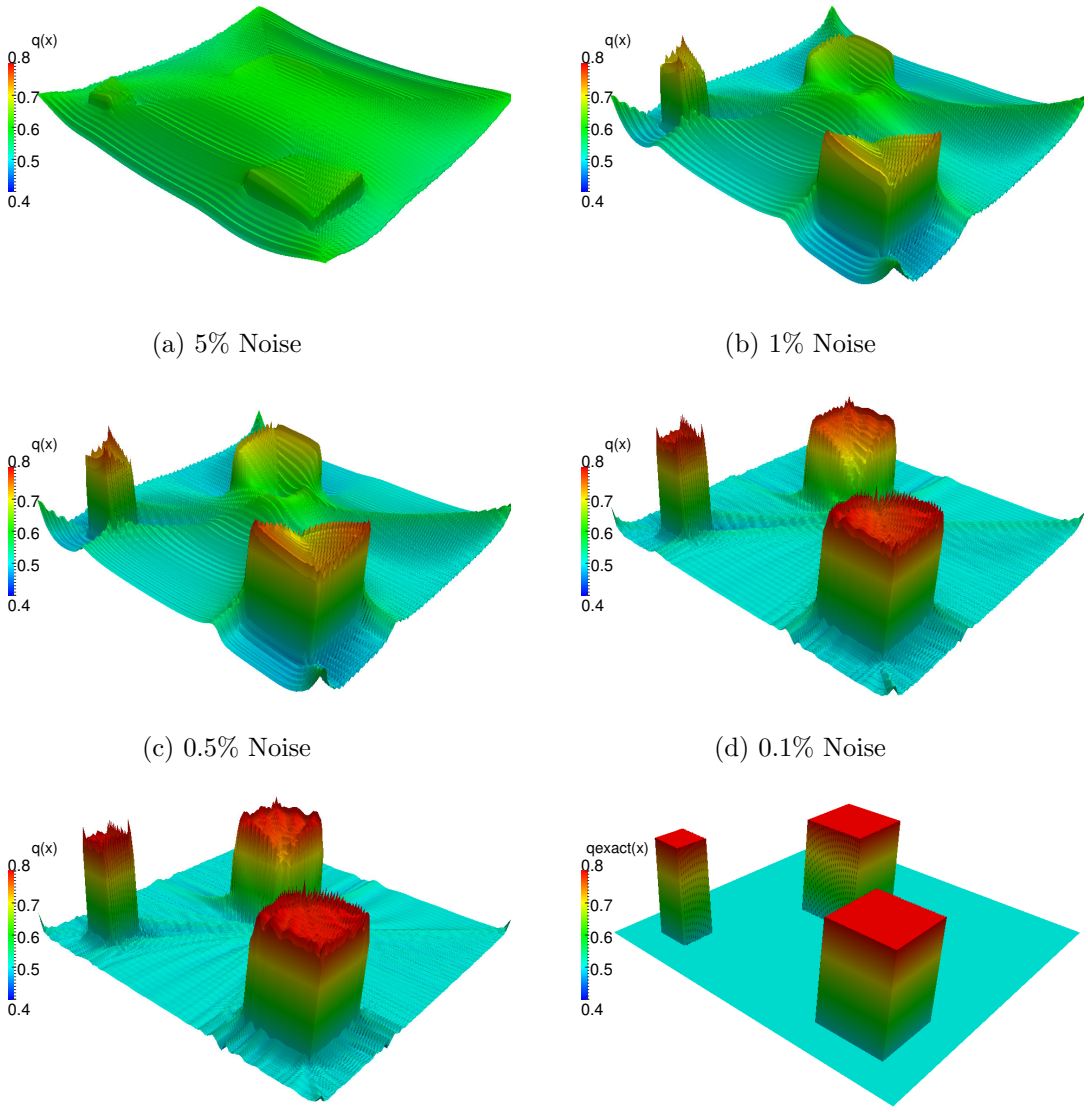


(a) 5% Noise

(b) 1% Noise

(c) 0.5% Noise

(d) 0.1% Noise

(e) 0.05% Noise

(f) Exact $q(x)$

Figure 4.5: Exact and reconstructed solutions for different noise levels

With noise levels greater than 1%, the reconstruction is very bad and the guess of $q_{guess}(x) = 0.6$ dominates. This is due to the large reconstruction parameter $\alpha$ chosen by the Discrepancy Principle.

The reason for the poor performance of Morozov's Discrepancy Principle in this case is that the smoothness assumption on the solution of the inverse problem is violated.

### 4.1.3 Localized slow convergence of the CG method

The reconstructions showed very slow convergence in the middle of the domain for both coefficients. Even for small noise levels, there is an intersection of rays near the center. Along these rays, the CG method converges very slowly.

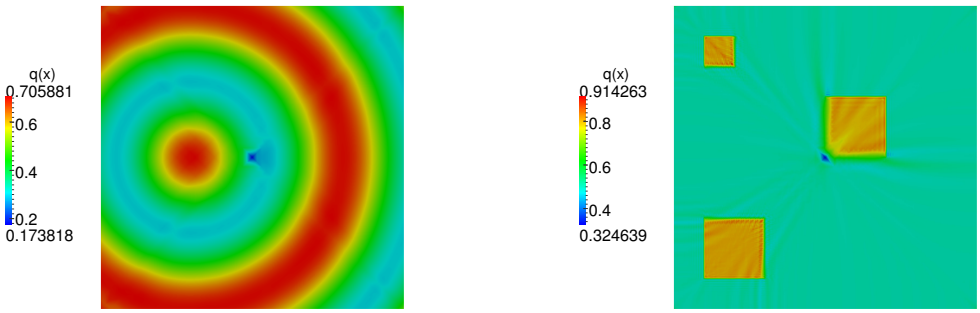


(a) Smooth coefficient (b) Non-smooth coefficient

Figure 4.6: Both coefficients at $\delta = 1.e-4$

The nonlinear conjugate gradient method needs many more steps before these rays get smaller. Requiring this small additional accuracy would result in a very long runtime with little benefit.

A possible reason for this behavior was already mentioned in the introduction: In the 1D problem, the coefficient was given by

$$q(x) = -\frac{F(x)}{u'(x)}$$

and therefore, even small noise can make it impossible to find $q(x)$ where $u'(x) \approx 0$. Looking at the exact forward solutions $U(q)$, one sees that there is a maximum near the center in both cases, resulting in $|\nabla u(x)| \approx 0$ in that neighborhood. It could be a coincidence that the peaks in the coefficients and the maxima of the forward solutions both appeared near the center. Therefore, this is investigated further.

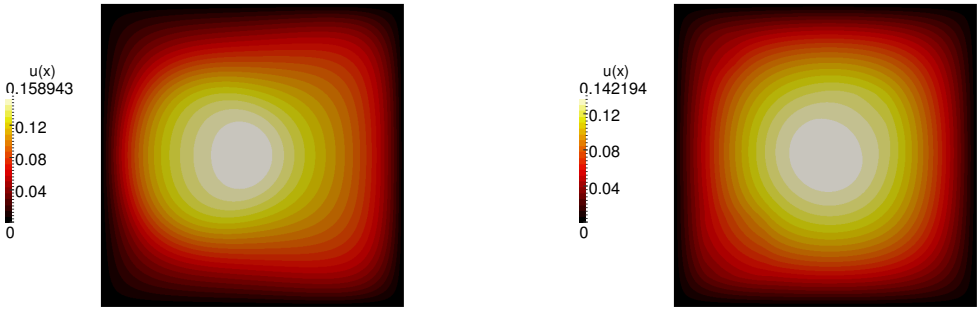


(a) $u(q)$ for smooth coeff. (b) $u(q)$ for non-smooth coeff.

Figure 4.7: Exact forward solutions for both coefficients

In order to verify the hypothesis above, a different load function is used. The function $f(x) = 1$ is replaced by

$$f(x) = \begin{cases} 3 & \text{if } x \in [0.5, 1]^2 \\ \frac{1}{3} & \text{else} \end{cases}$$

The goal being to relocate the maximum of the forward solutions $U(q)$, which now look as follows:

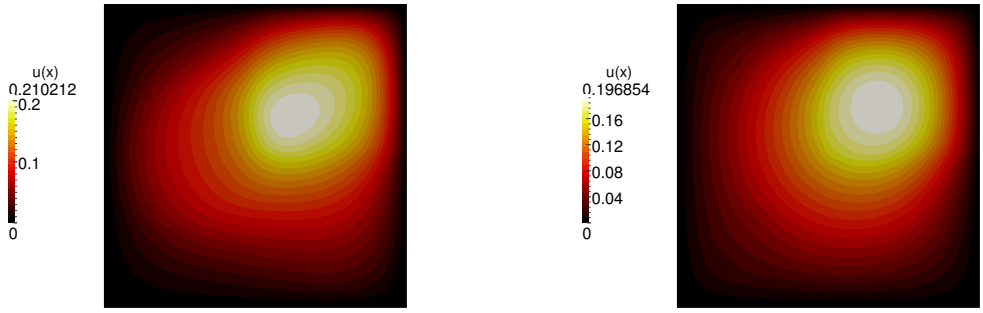


(a) $u(q)$ for smooth coeff. (b) $u(q)$ for non-smooth coeff.

Figure 4.8: Forward solutions for the new load function

It is of interest to see, whether this has an influence on the location of the intersection of the rays in the reconstructed coefficients, which look as follows:

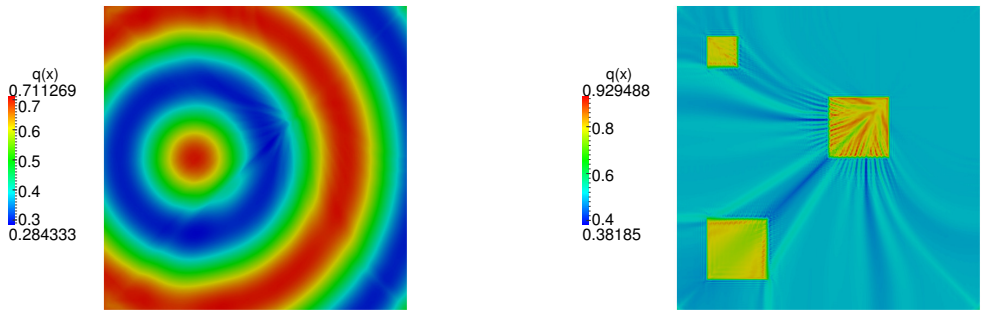


(a) Smooth coefficient (b) Non-smooth coefficient

Figure 4.9: Both coefficients at $\delta = 1.e - 4$ (new load function)

Now, the rays intersect more to the top-right. The intersections are again located at the maximum of their corresponding forward solution, where $|\nabla u(x)| \approx 0$. This strongly suggests that the rays and peaks result from the fact that the coefficient cannot be reconstructed where the gradient of $u$ vanishes.

### 4.1.4 Choice of Tikhonov parameter using the Discrepancy Principle

It is interesting to see whether there is an analytic relationship between the noise level $\delta$ and the Tikhonov parameter $\alpha$ chosen by the Discrepancy Principle in the experiments above and also, whether there is a difference between the smooth and the non-smooth coefficient.

The Tikhonov parameter $\alpha$ plotted against the corresponding noise level $\delta$ looks as follows:

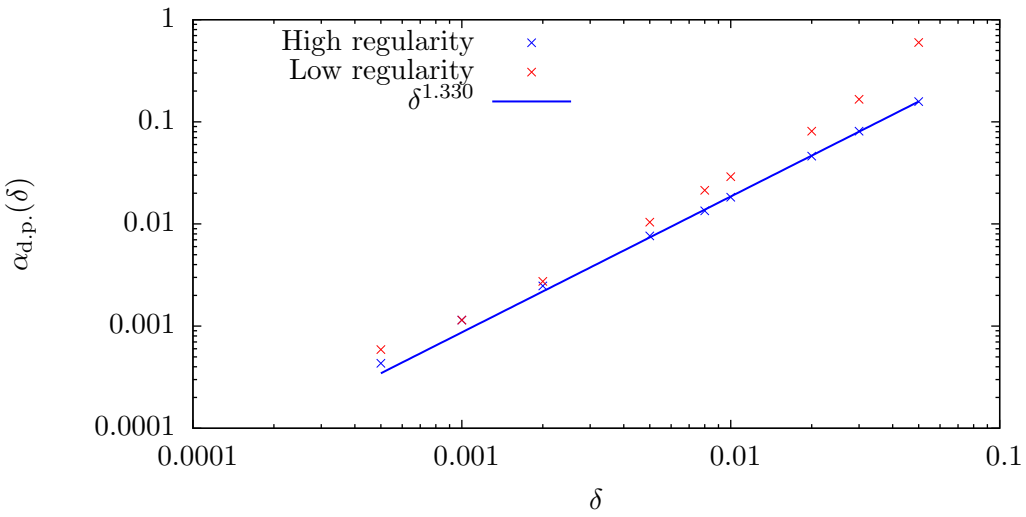


Figure 4.10: Reconstruction parameter chosen by the D.P. as a function of $\delta$

For the smooth coefficient the choices of $\alpha$ behave like a power law in $\delta$. The reconstruction parameters chosen in the non-smooth case do not show this behavior and they are always greater than the corresponding $\alpha$ for the smooth coefficient. This already shows that a good qualitative reconstruction cannot be expected for the low-regularity coefficient.

Also, the non-smooth coefficient with a noise level of 5% illustrates quite well that the continuous dependence of the solution on the data is not given: Despite the comparatively large reconstruction parameter, the residual is already small enough to fulfill the Discrepancy Principle, resulting in a reconstructed coefficient that is still very close to the initial guess (and far from the actual solution).

## 4.2 $H^1(\Omega)$-Tikhonov term

In this experiment, the $L^2(\Omega)$-Norm of the Tikhonov term is replaced by the $H^1(\Omega)$-Norm. This change of (2.4.0.1) results in the following new functional to be minimized by the nonlinear CG method:

$$\hat{J}(q) = \frac{1}{2}\int_\Omega q(x)|\nabla(U(q) - u^\delta)|^2 dx + \frac{\alpha}{2}\|q - q^\star\|^2_{H^1(\Omega)} \tag{4.2.0.1}$$

The idea behind using this new functional is that, due to the smoothing property of the $H^1$-term, the peaks and rays observed in the previous experiments should become less pronounced or even disappear altogether.

The problem with this functional is that it seems to be much harder to minimize, as the CG method takes much longer to converge. Therefore, the calculations were carried out on a mesh of $\Omega = [0,1]^2$ with $N = 8'321$ instead of $N = 33'025$. In order to be able to compare the results, the experiments using the $L^2(\Omega)$-Tikhonov term are carried out on this mesh as well.

Since the $H^1(\Omega)$ regularization is much stronger than $L^2(\Omega)$, the Discrepancy Principle parameter $\tau$ is adjusted to $\tau = 1.2$. For the $L^2$-case, it is still set to 2.5.

The convergence rates in the $L^2(\Omega)$-Norm for this new functional with respect to the noise level $\delta$ looks as follows:

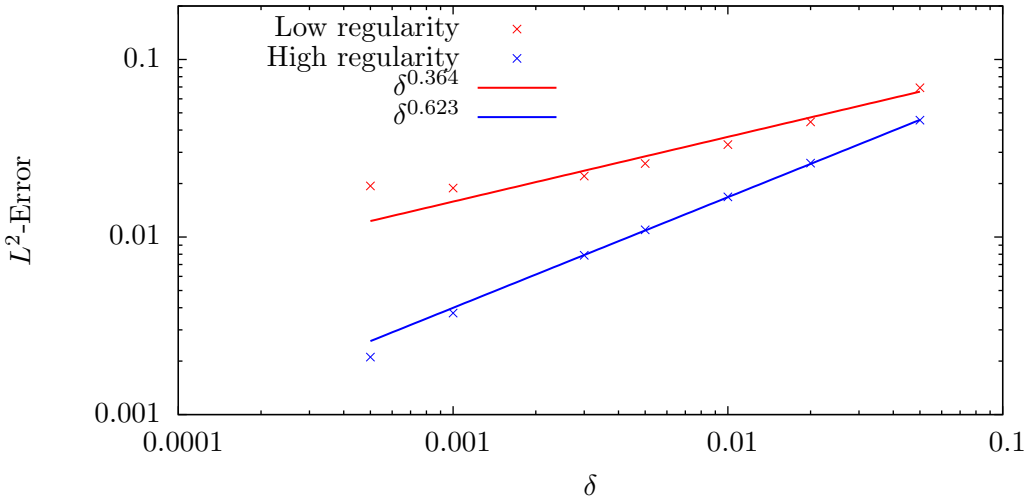


Figure 4.11: New functional: Convergence in $L^2(\Omega)$

The striking difference to the previous experiments is that for very low noise levels, the low regularity reconstruction gets worse. This is most likely due to the fact that the reconstructed coefficients are smooth, unlike the exact solution in this case. For the smooth coefficient one observes even better convergence, since the additional smoothening introduced by the new Tikhonov term works in favor of the reconstruction.

Although these convergence plots do not look very promising, the quantitative and qualitative reconstructions are actually better, even for the non-smooth coefficient: The convergence rates may be about equal, but the errors are smaller over all, which can be seen in a direct comparison between the two functionals (2.4.0.1 and 4.2.0.1) and their respective convergence fits:

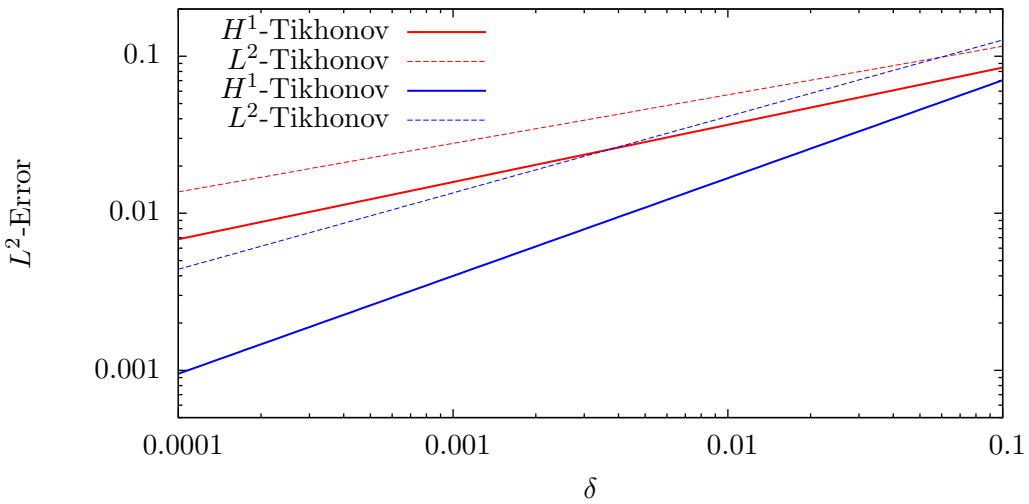


Figure 4.12: Convergence in $L^2(\Omega)$: Comparison between the two functionals

This can be observed qualitatively by comparing the following 3D plots of the reconstructed

coefficients for both functionals. First, the high-regularity coefficient:

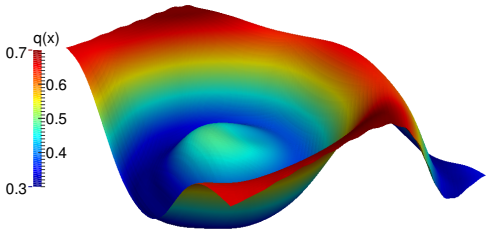


(a) $H^1$-Tikhonov for $\delta = 5\%$

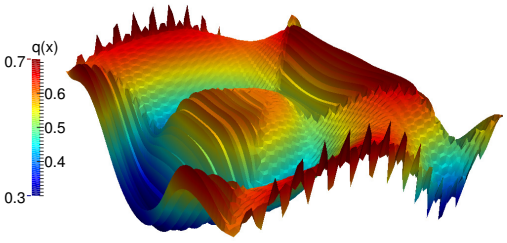


(b) $L^2$-Tikhonov for $\delta = 5\%$

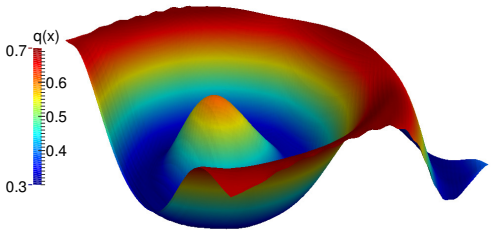


(c) $H^1$-Tikhonov for $\delta = 1\%$

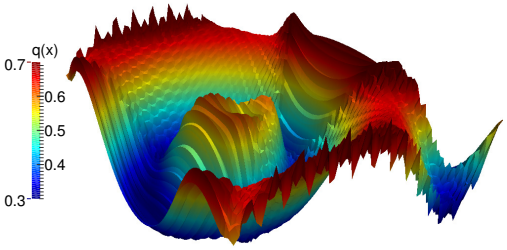


(d) $L^2$-Tikhonov for $\delta = 1\%$

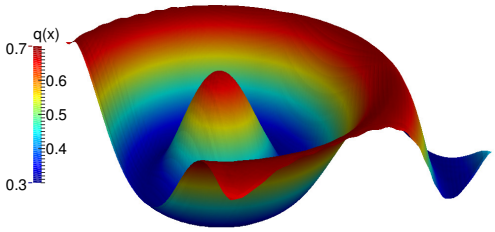


(e) $H^1$-Tikhonov for $\delta = 0.1\%$

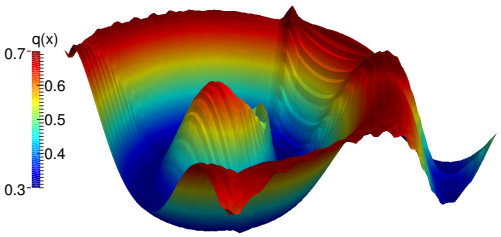


(f) $L^2$-Tikhonov for $\delta = 0.1\%$

Figure 4.13: Comparison of the two functionals for the high-regularity coefficient

The reconstructions for the low-regularity coefficient also look a lot better when using the $H^1(\Omega)$-Tikhonov term:

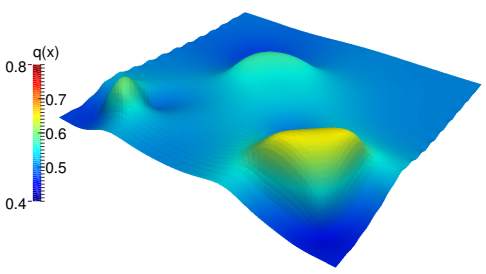


(a) $H^1$-Tikhonov for $\delta = 5\%$

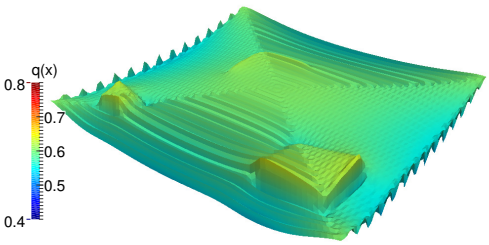


(b) $L^2$-Tikhonov for $\delta = 5\%$

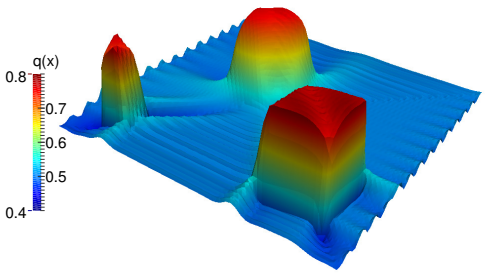


(c) $H^1$-Tikhonov for $\delta = 1\%$

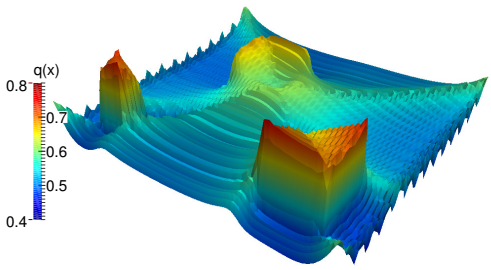


(d) $L^2$-Tikhonov for $\delta = 1\%$

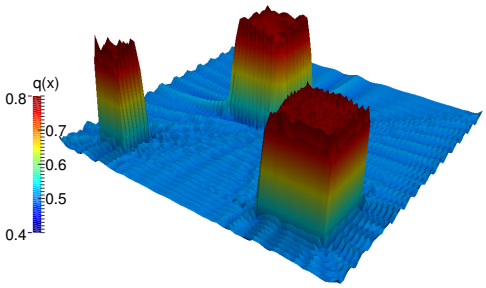


(e) $H^1$-Tikhonov for $\delta = 0.1\%$

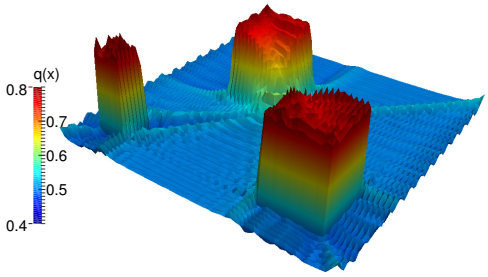


(f) $L^2$-Tikhonov for $\delta = 0.1\%$

Figure 4.14: Comparison of the two functionals for the low-regularity coefficient

The solutions associated with the $L^2(\Omega)$-Tikhonov term show strong oscillations, which result from the high-frequency measurement-noise. The smoothing property of the $H^1(\Omega)$-Norm takes care of these, allowing to choose the Discrepancy Principle parameter $\tau$ much smaller, without getting solutions that are dominated by these oscillations. This results in more accurate reconstructions both quantitatively and qualitatively.

# Chapter 5

# Summary

The inverse coefficient problem of determining $q \in Q \subset L^\infty(\Omega)$ such that the Poisson equation is satisfied in a weak sense was implemented successfully in c++ using the Distributed and Unified Numerics Environment (DUNE) and the Pardiso linear solver.

The search for the minimizer of the energy functional from [1] was implemented using a nonlinear conjugate gradient method. The gradient of the functional was determined with the adjoint-state method. A disadvantage of using CG is the slow convergence on rays from the boundary to where $\nabla u(x) \approx 0$, which could be solved by requiring more accuracy or by using an $H^1(\Omega)$-Tikhonov term, both resulting in longer run times. An advantage of CG is that it does not require the Hessian, which allows solving much bigger problems since no dense matrix operations are required.

The experiments performed with the resulting code were in good agreement with the theory of nonlinear ill-posed operator equations: Good convergence in the noise level was observed for smooth coefficients, i.e. $O(\sqrt{\delta})$, and slow convergence for non-smooth coefficients. This was expected since the discrepancy principle, which was used as a parameter choice rule, requires a certain degree of smoothness to be order-optimal. Also, when using an $H^1(\Omega)$-Tikhonov term (instead of $L^2(\Omega)$), the reconstructions got better, at the cost of longer run times.

# References


[1] Dinh Nho Hào and Tran Nhan Tam Quyen. Convergence rates for tikhonov regularization of coefficient identification problems in laplace-type equations. *Inverse Problems*, 26(12):125014, 2010.

[2] Ralf Hiptmair. *Lecture: Numerical Methods for Partial Differential Equations*. ETH Zurich, 2013.

[3] Rene Pinnau and Michael Ulbrich. *Optimization with PDE constraints*, volume 23. Springer, 2008.

[4] Andreas Rieder. *Keine Probleme mit Inversen Problemen*, volume 1. Vieweg Wiesbaden, 2003.

[5] O. Scherzer. The use of morozov's discrepancy principle for tikhonov regularization for solving nonlinear ill-posed problems. *Computing*, 51(1):45–60, 1993.